Ovine herpesvirus 2 encodes a previously unrecognized protein, pOv8.25, that targets mitochondria and triggers apoptotic cell death

Shrestha, Neeta ; Tobler, Kurt ; Uster, Stephanie ; Sigrist-Nagy, Romina ; Hierweger, Melanie Michaela ; Ackermann, Mathias

Abstract: Malignant catarrhal fever (MCF) is a rare but frequently lethal disease of certain cloven-hoofed animals. At least 10 different viruses, all members of the macavirus genus in the subfamily gammaherpesvirinae, are known as causative agents of MCF. Among these, Ovine herpesvirus 2 (OvHV-2) is the most frequent and economically most important MCF agent. Phenotypically, MCF is characterized by severe lymphocytic arteritis-periarteritis, which leads to the accumulation of activated lymphocytes, accompanied by apoptosis and necrosis in a broad range of tissues. However, a viral factor that might be responsible for the tissue damage has not yet been identified. We have studied a seemingly intergenic locus on the OvHV-2 genome, which had previously been shown to be transcriptionally highly active in MCF-affected tissue. We identified by 5'- and 3' RACE a conserved, double-spliced transcript that encoded for a 9.9 kDa hydrophobic protein. The newly detected gene, Ov8.25, and its splicing pattern was conserved among OvHV-2 strains from different origins. Upon transient expression of synthetic variants of this gene in various cell types, including bovine lymphocytes, the protein (pOv8.25) was shown to targeting the mitochondria, followed by caspase-dependent apoptosis and necrosis. Notably, a deletion mutant of the same protein lost these abilities. Finally, we detected pOv8.25 in brain-infiltrating lymphocytes of cattle with MCF. Thus, the cell-death causing properties of pOv8.25 in affected cells may be involved in the emergence of typical MCF-associated apoptosis and necrosis. Thus, we have identified a novel OvHV-2 protein, which might contribute to the phenotype of MCF-related lesions.IMPORTANCEOvine herpesvirus 2 (OvHV-2) circulates among sheep without causing disease. However, upon transmission to cattle, the same virus instigates a frequently lethal disease, Malignant catarrhal fever (MCF). While cause of death and pathogenesis of tissue lesions are still poorly understood, MCF is characterized by accumulation of lymphocytes in various tissues, associated with vasculitis and cell death. As infectious virus is hardly present in those lesions, the cause of cell death cannot simply be explained by viral replication. The significance of our research is in identifying and characterizing a previously overlooked gene of OvHV-2 (Ov8.25), which is highly expressed in animals with MCF. Its encoded protein targets mitochondria, causing apoptosis and necrosis, thus, contributing to understand the source and nature of cell death. As the corresponding genetic locus is also active in the context of MCF due to a different Macavirus, we may have detected a common denominator of the disease phenotype.

DOI: https://doi.org/10.1128/JVI.01536-19

Originally published at:
Shrestha, Neeta; Tobler, Kurt; Uster, Stephanie; Sigrist-Nagy, Romina; Hierweger, Melanie Michaela; Ackermann, Mathias (2020). Ovine herpesvirus 2 encodes a previously unrecognized protein, pOv8.25, that targets mitochondria and triggers apoptotic cell death. Journal of Virology, 94(8):e01536-19.
DOI: https://doi.org/10.1128/JVI.01536-19

Ovine herpesvirus 2 encodes a previously unrecognized protein, pOv8.25, that targets mitochondria and triggers apoptotic cell death

Running title: Ov8.25 protein and MCF pathogenesis

Authors: Neeta Shrestha[1a], Kurt Tobler[1], Stephanie Uster[1b], Romina Sigrist-Nagy[1c], Melanie Michaela Hierweger[2], Mathias Ackermann[1]*

[1]Institute of Virology, Vetsuisse Faculty, University of Zurich, Zurich, Switzerland

[2]Division of Experimental Clinical Research, Vetsuisse Faculty, University of Bern, Bern, Switzerland

*Contact: Mathias Ackermann, Institute of Virology, VSF, University of Zurich, Winterthurerstrasse 266a, CH-8057 Zurich, Switzerland. Phone: +41 44 635 87 01, email: mathias.ackermann@uzh.ch

Author Contributions: Conceptualization, M.A., N.S., K.T; data curation, N.S. and M.A.; formal analysis, N.S., S.U., K.T, R.S., M.M.H., M.A.; funding acquisition, M.A.; investigation, N.S., S.U., R.S., M.M.H.; methodology, N.S., K.T., M.M.H., M.A.; project administration, M.A.; resources, M.A.; supervision, K.T., M.A.; validation, N.S., K.T., M.A.; visualization, N.S., M.A., S.U., R.S., M.M.H.; writing—original draft, M.A., N.S., S.U., K.T., R.S; writing—review and editing, M.A.

[a] Present address: Division of Experimental Clinical Research, Vetsuisse Faculty, University of Bern, Bern, Switzerland
[b] Present address: The Institute for Infectious Diseases, Medical Faculty, University of Bern, Bern, Switzerland
[c] Present address: Felsberg, Switzerland

Abstract

Malignant catarrhal fever (MCF) is a rare but frequently lethal disease of certain cloven-hoofed animals. At least 10 different viruses, all members of the *macavirus* genus in the subfamily *gammaherpesvirinae*, are known as causative agents of MCF. Among these, Ovine herpesvirus 2 (OvHV-2) is the most frequent and economically most important MCF agent. Phenotypically, MCF is characterized by severe lymphocytic arteritis-periarteritis, which leads to the accumulation of activated lymphocytes, accompanied by apoptosis and necrosis in a broad range of tissues. However, a viral factor that might be responsible for the tissue damage has not yet been identified. We have studied a seemingly intergenic locus on the OvHV-2 genome, which had previously been shown to be transcriptionally highly active in MCF-affected tissue. We identified by 5'- and 3' RACE a conserved, double-spliced transcript that encoded for a 9.9 kDa hydrophobic protein. The newly detected gene, Ov8.25, and its splicing pattern was conserved among OvHV-2 strains from different origins. Upon transient expression of synthetic variants of this gene in various cell types, including bovine lymphocytes, the protein (pOv8.25) was shown to targeting the mitochondria, followed by caspase-dependent apoptosis and necrosis. Notably, a deletion mutant of the same protein lost these abilities. Finally, we detected pOv8.25 in brain-infiltrating lymphocytes of cattle with MCF. Thus, the cell-death causing properties of pOv8.25 in affected cells may be involved in the emergence of typical MCF-associated apoptosis and necrosis. Thus, we have identified a novel OvHV-2 protein, which might contribute to the phenotype of MCF-related lesions.

IMPORTANCE

Ovine herpesvirus 2 (OvHV-2) circulates among sheep without causing disease. However, upon transmission to cattle, the same virus instigates a frequently lethal disease, Malignant catarrhal fever (MCF). While cause of death and pathogenesis of tissue lesions are still poorly understood, MCF is characterized by accumulation of lymphocytes in various tissues, associated with vasculitis and cell death. As infectious virus is hardly present in those lesions, the cause of cell death cannot simply be

explained by viral replication. The significance of our research is in identifying and characterizing a previously overlooked gene of OvHV-2 (Ov8.25), which is highly expressed in animals with MCF. Its encoded protein targets mitochondria, causing apoptosis and necrosis, thus, contributing to understand the source and nature of cell death. As the corresponding genetic locus is also active in the context of MCF due to a different Macavirus, we may have detected a common denominator of the disease phenotype.

Key words: Malignant catarrhal fever, MCF, Herpesvirus, Macavirus, Ovine herpesvirus 2, OvHV-2, Ov8.25, pathogenesis, apoptosis, necrosis, mitochondria, disease phenotype.

Introduction

Malignant catarrhal fever (MCF) is a rare but frequently lethal disease, affecting various species in the order *Artiodactyla* (even-toed cloven-hoofed animals). Two related viruses, Alcelaphine herpesvirus 1 (AlHV-1) and Ovine herpesvirus 2 (OvHV-2), both belonging to the *macavirus* genus within the subfamily *gammaherpesvirinae*, are responsible for most cases of MCF, although at least 8 additional MCF-causing viruses are known (reviewed in (1)). The economically most important form of MCF affects cattle as well as farmed bison and deer, occurs worldwide, and is associated to OvHV-2. AlHV-1 also affects cattle but is restricted predominantly to Africa and to zoos (2-4). Typically, there are two types of host for the same virus, a reservoir host, among which the virus circulates without causing disease symptoms, and an indicator host, which is usually free of the same virus but succumbs to MCF upon accidental infection (1, 5-9). In the case of OvHV-2, sheep are the reservoir host, while the main range of indicator hosts includes various members of the *bovinae*, including cattle, water buffaloes and bison; the *cervidae*, including red deer and sika deer; the *suidae*, including the domestic pig (6, 10-17).

Various clinical forms of the disease have been described but the so called “head and eye form” is most common, with typical signs including fever, inappetence, ocular and nasal discharge, corneal opacity, mucosal lesions in the buccal and nasal cavities and around the muzzle, diarrhea and depression. Up to 95% of affected cattle succumb to death or have to be euthanized within one week after the onset of the disease (6, 8, 12). Histologically, MCF is characterized by the accumulation of lymphocytes, apoptosis and necrosis in a range of tissues but the morphological hallmark is severe lymphocytic arteritis-periarteritis with affection of the tunica media (8, 18, 19).

While viral transmission, clinical signs and histopathological changes associated with the disease have been well characterized, major aspects of the pathogenesis of MCF are still enigmatic. It is agreed, however, that both viral and host determinants play a role. Among the viral factors involved, it has been shown at least for AlHV-1 that expression of the latency-associated nuclear antigen (LANA) plays an essential role because a LANA-knock-out virus did not induce MCF (20). Based on this observation, it has been concluded that the infecting virus must be able to establish a latent infection

prior to the outbreak of the disease. However, the predicted properties associated to the LANA protein, which include maintenance of the viral genome during latency, cannot explain the disease phenotype. In the context of OvHV-2 such experiments have not yet been feasible because the virus can neither be propagated in conventional cell cultures nor is an infectious BAC-clone available that would make genetic engineering of the viral genome possible. However, there is ample evidence available, suggesting that the LANA gene (ORF73) is also expressed during MCF due to OvHV-2 (21). In addition, various reports have detected expression of OvHV-2 lytic genes throughout the course of the disease (22, 23). It has been debated, therefore, whether the lytic or the latent OvHV-2 may be responsible for the outbreak of MCF. As animals suffering from MCF typically do not shed and transmit the virus, it has also been agreed that OvHV-2 replicates only poorly in the indicator animal species (1, 8, 24). Therefore, viral replication plays certainly an important role at very early stages of the infection, particularly prior to dissemination within the body. However, at later times, viral lytic genes may be transcribed and translated but certainly will not yield high viral titers. Indeed, typical herpesviral particles cannot consistently be found in affected tissues of animals with MCF but can be readily detected in nasal sheddings of seemingly healthy sheep excreting OvHV-2 (25, 26). Overall, no common denominator has yet been identified among the Macaviruses that might explain the occurrence and disease phenotype of MCF.

In previous work, we have detected a genetic locus within the OvHV-2 genome with high transcriptional activity in lymphatic tissue of animals with SA-MCF (21). Interestingly, the same region in AlHV-1 was also transcriptionally active in tissues from animals with experimental AlHV-1 derived MCF (20). Hitherto, no gene has been allocated to this transcript, although the region in AlHV-1 has been designated E16 or ER16 (ER for expressed region), whereas we referred to the corresponding region in OvHV-2 as “intergenic” (20, 21). In the present work, we have mapped a previously overlooked viral gene, newly designated as Ov8.25, to this region, noting that it gives rise to a double-spliced mRNA, which translates into a small, hydrophobic protein. Transient expression of this protein (pOv8.25) showed that it targeted the mitochondria,

causing apoptosis and necrosis in transfected cells. Finally, pOv8.25 was also detected in the brain of cattle with MCF.

Results

Sequence of a novel transcript expressed in OvHV-2-infected cells

In previous work (21), an RNA mapping to a seemingly intergenic region of the OvHV-2 genome had been detected by microarray analysis in lymphnodes of cows with MCF. Here, RNA was extracted from two different sources in order to identify the ends of the predicted molecule by 5'-RACE and 3'-RACE as described in Materials and Methods. The first RNA-template originated from lymphocytes of a cow with MCF. The second RNA-template was extracted from OvHV-2-infected large granular lymphocytes (LGLs).

The products of the RLM-RACE PCR were loaded on a 1% agarose gel (Fig. 1). After nested amplification, the 5`end provided a product of approximately 400 bp (lane 4), whereas the 3`end resulted in a 200 bp product (lane 2). Similar results were obtained with the second template (data not shown).

The PCR products were cloned using the TOPO-TA method and submitted for sequencing. Interestingly, the sequences obtained from the two independent sources were 96% identical. The sequences were then aligned to the OvHV-2 genomes published in GenBank (AY839756, a Scotch strain, derived from bovine LGLs; DQ198083, an American strain, derived from sheep nasal secretions). The 5'-end of the transcript from the cow with MCF mapped to position 114706 of the Scotch strain, which corresponds to position 114555 of the American strain. The 3'-end mapped to the positions 115450 (Scotch strain) and 115287 (American strain), respectively. From these map positions, a transcript size of between 745 (Scotch strain) and 733 bases (American strain) could be predicted. However, the observed transcript size was less. It was also evident that there were two parts in the OvHV-2 genomes, which were not detected in the transcripts. The most probable explanation for these gaps was a splicing process executed on the primary transcript. Indeed, upon *in silico* analysis of the transcript's sequence, the NetGene2 Server confirmed the observed splice sites with

good statistical confidence (www.cbs.dtu.dk/services/NetGene2) (see Fig. 2). Significantly, the predicted splice sites were conserved in all four sequences.

The novel transcript is spliced upon transient expression

The genomic locus encompassing the two putative introns was amplified by PCR and cloned under the control of the cmvIE promoter into the pEGFP N3 vector for transient expression assays. HEK 293T cells were transfected with this construct and total RNA was harvested at 25 hrs post transfection. After reverse transcription, the cDNA was PCR amplified by using primers corresponding to the terminal OvHV-2 sequences of the construct. Input DNA was used as a positive control. Fig. 3 shows the results. The DNA template provided a PCR product of just below 400 bp, which corresponded well with the expected size of 364 bp (lane 5). In contrast, the cDNA template (lanes 2, 3, 4) provided one strong band at approximately 200 bp and two weaker bands; the upper migrating as the unspliced DNA template and the second at an intermediate position, just below 300 bp. The strong band was consistent with the predicted size (177 bp) of the double-spliced transcript, which was verified by extracting the band from the gel followed by sequencing. The intermediate band may represent a single-spliced variant. Thus, splicing of the transiently expressed transcript took place, even in the absence of other factors contributed by OvHV-2. Based on these results, we concluded that the afore-mentioned "intergenic" region of the OvHV-2 genome was by no means "intergenic". Rather, it comprised a thus far overlooked OvHV-2 gene. BLAST analysis did not reveal similar genes in other herpesviruses. Therefore, we considered it as an OvHV-2-specific gene. Due to its location on the OvHV-2 genome, in between ORF69 and Ov8.5, the novel gene was named Ov8.25.

Ov8.25 encodes a protein

To address the novel gene's capacity to encode for a protein, the afore-mentioned cDNA was PCR amplified by using primers that targeted the Ov8.25 sequence beginning from the predicted ATG of the putative open reading frame (ORF) down to the 3'-end of the ORF but without the STOP codon. This amplified sequence was then

cloned into an HSV-1 amplicon vector, which also provided a C-terminal yellow fluorescence protein (EYFP) as a fusion partner for the putative Ov8.25 protein. The resulting construct was transfected into Vero 2-2 cells and analyzed under the fluorescence microscope at 24 hrs post transfection. As shown in Fig. 4A, an EGFP-expressing control amplicon construct illuminated the body of transfected cells with green fluorescent protein. In contrast, as shown in Fig. 4B, the putative pOv8.25-EYFP-fusion protein localized to the cytoplasm, predominantly around the rim of the cellular nucleus. It was noted that cells expressing the newly detected protein showed quite often an enlarged nucleus. Moreover, the yield of pOv8.25 protein seemed to be low.

Splicing of the Ov8.25 transcript is independent of its protein-coding sequences

The putative function of the Ov8.25 locus might be associated either to the encoded protein or to splicing of the primary transcript or else even to both features. In order to discriminate between these possibilities, synthetic constructs as described in Tab. 3 were generated. The five constructs were separately transfected into Vero 2-2 cells and RNA was harvested after 24 hrs. Each RNA extract was reverse transcribed into cDNA before amplifying the sequences of interest by PCR as described in Materials and Methods. As shown in Fig. 5., the transiently expressed transcript was spliced even when the amino acid coding sequences had been optimized for translation in Bovine cells (lane 3) or when protein translation was abolished after removing all start codons (ATG) from within the coding sequences and replacing them by stop codons (lane 6). The same extracts amplified without prior treatment with reverse transcriptase (lanes 4 and 7) did not yield a product. In contrast, when the corresponding plasmid DNA was used as PCR template, a larger band became visible (lanes 2 and 5), where the size difference could be explained by the size of the introns. Similarly, the single intron constructs were spliced as shown in lanes 9 and 12 (corresponding controls in lanes 8, 10 and 11, 13, respectively). In contrast to all of those constructs, the synthetic intronless construct remained unspliced (lanes 15 to 17).

Primary characterization of the pOv8.25-EYFP fusion protein

According to its amino acid sequence and although it did not feature a signal sequence, the Ov8.25 protein (pOv8.25) was predicted to be a membrane protein (Fig. 6) with two transmembrane domains and a predicted molecular weight of 9.9 kDa. In the absence of existing antibodies against pOv8.25, the encoded translation product was first characterized as a EYFP fusion protein.

To this end, Vero 2-2 cells were transfected with amplicon vectors encoding either EYFP alone or EYFP as C-terminal fusion protein to pOv8.25. 24 hrs after transfection, yellow fluorescence was observed in approximately 50% of the cells, which were then harvested for analysis by Western immunoblot using a monoclonal antibody against GFP (Fig. 7A). EYFP was expected to migrate at approximately 26,9 kDa and the pOv8.25-EYFP fusion protein at 38,8 kDa. However, a second, faster migrating band of approximately 33 kDa was visible in lane 2 but absent in lane 3. The size of this 33 kDa band corresponds well to the predicted molecular weight of an N-terminally truncated Ov8.25-EYFP fusion protein, whose translation would start only at the second methionine-codon (position M51). Such a truncation would remove the predicted transmembrane domains of pOv8.25, which might interfere with its subcellular localization and biological function. Interestingly, also slower migrating bands at about 70 kDa were stained by the anti-GFP antibody in each of the two Ov8.25-transfected extracts in lanes 2 and 3 (Fig. 7A). The same extra bands were also visible in the insoluble extract (Fig. 7B), where, even an additional 48 kDa band emerged. These higher bands were not visible in the EYFP extract, the non-transfected cell extract (lane 4), or the soluble cell extracts (Fig. 7C). The nature of these bands cannot yet be rationally explained. Yet, potential reasons may include dimerization or covalent binding to a host protein.

In order to address the nature of the 33 kDa band that was only visible in extracts from cells transfected with the codon-optimized, intronless Ov8.25 coding sequence, two 5'-deletion mutants were constructed, one yielding a 5'-truncated codon-optimized Ov8.25 locus with C-terminal EYFP, the other giving a 5'-truncated codon-optimized, intronless Ov8.25 coding sequence with C-terminal EYFP. Both constructs had their translation

initiation codon at the previous position 51 (M51, see Fig. 6), which caused a loss of the membrane anchoring of the truncated protein. Accordingly, we hypothesized that the truncated proteins may be more soluble than their original counterparts. To address this issue, cells were transfected with either the original constructs or their truncated counter parts. Non-transfected cell and cells transfected with the EYFP amplicon served as controls. After harvesting, the cells were suspended in a buffer containing Triton X-100 before soluble and insoluble components were separated by centrifugation. Soluble and insoluble extracts were separated by SDS-PAGE, transferred to Western blots and stained using the anti-GFP mcAb. The results are shown in Fig. 7, panels B and C. By itself, EYFP divided almost uniformly into the soluble and the insoluble fractions (lanes 2 in panels B and C). However, a fainter and faster migrating band was additionally observed in the soluble fraction (lane 2, panel C). In contrast, the full length Ov8.25 fusion proteins accumulated predominantly in the insoluble fraction (lanes 3, 4 in panel B). Indeed, the high molecular weight bands were readily detected in the insoluble fractions but invisible in the soluble fractions (lanes 3, 4 in panel C). However, the predicted 38,8 kDa band was discernible in both fractions. Interestingly, the M51-truncated proteins were not detected in the insoluble fractions (lanes 5 and 6 in panel B) but were readily discernible among the soluble proteins (lanes 5 and 6 in panel C). The 33 kDa protein produced in cells transfected with the codon-optimized, intronless Ov8.25 coding sequence was not seen among the insoluble proteins (lane 4 in panel B) but sided entirely to the soluble fraction (lane 4 in panel C). Moreover, it migrated at the same velocity as the truncated versions of pOv8.25, which was consistent with the hypothesis that it actually represented a secondary translation product of the codon-optimized fusion protein, which used M51 as its start codon. Since actin, shown in panel A' migrated very close to the fusion proteins of interest, we used the slower migrating tubulin as a loading control. The blots B and C were re-stained, using a monoclonal antibody against tubulin. The immunoblots B' and C' clearly demonstrate that a major part of tubulin went into the soluble fraction, although enough tubulin was retained in the insoluble fraction to show that comparable amounts of cell extracts had been loaded in each lane.

Identification of the Ov8.25 protein by antibodies to synthetic peptide

To open the possibility of recognizing the Ov8.25 protein in its native form, without tag, rabbits were immunized with a synthetic peptide, which had been predicted to represent an immunogenic part of pOv8.25, namely spanning from aa 60 to 76 of the predicted protein (see Fig. 6). Vero cells were transfected either with the EYFP amplicon or the codon-optimized, intronless Ov8.25 coding sequence with C-terminal EYFP or the codon-optimized Ov8.25 locus with C-terminal EYFP or, as a negative control, they were left untransfected. Furthermore, the truncated versions of the two Ov8.25 fusion proteins were also included in the experiment. After 24 hrs, the cells were harvested and the insoluble fractions were subjected to SDS-PAGE and Western transfer. Identical blots were either immunostained with the rabbit anti-pOv8.25 peptide serum or with anti-GFP mcAb. The results are shown in Fig. 8. As expected, the rabbit anti peptide serum (panel A) was able to stain the predicted 38.7 kDa pOv8.25-EYFP fusion proteins (lanes 3, 4) but did not react with EYFP alone (lane 2) or with non-transfected Vero cells (lane 1). As expected, the truncated forms of pOv8.25 were not detected on the blot, since they had been removed with the soluble fractions.

Moreover, the rabbit anti-peptide serum recognized also the higher molecular bands in lanes 3 and 4 of panel A, the one migrating just above 70 kDa. Bands of much the same sizes were also recognized by the anti-GFP mcAb in lanes 3 and 4 (panel B). Importantly, the rabbit anti-peptide serum did no longer react with the same proteins if it was saturated with the immunizing peptide (panel C). Together, these data suggest that the anti-peptide serum actually recognized the pOv8.25-fragment of the fusion protein and that this protein existed in at least two forms in transfected cells, namely in a monomeric form with the expected size of 38.7 kDa and in higher molecular forms of >70 respectively.

The pOv8.25-EYFP fusion protein targets mitochondria

As the pOv8.25 protein had been observed to assume a cytoplasmic localization (Fig. 4), it was of interest to know, where exactly this could be. Analysis of its amino acid sequence (Fig. 6) did reveal two potential transmembrane domains (aa 13-32 and aa 37-56). Moreover, a BPD_transp_1 domain had been predicted for aa 9 to 31. All of this

297 *in silico* information suggested that pOv8.25 may represent a membrane protein,
298 although a classical signal sequence was not identified.
299 Confocal microscopy was used to address this issue. Vero cells were transfected with
300 Ov8.25-EYFP amplicon DNA. Separate samples were harvested at 6, 24, and 48 hrs
301 post transfection and stained with fluorescent markers for individual membranous
302 compartments, i.e. Mitotracker to test co-localization with mitochondrial membranes,
303 ConA to make the ER compartment visible, and WGA to visualize the Golgi
304 membranes. As shown in Fig. 9, pOv8.25-EYFP (panels A,C and D,F) co-localized with
305 the mitotracker stain (panels B,C and E,F), which was corroborated by reconstructing
306 the three-dimensional structure of the cell (panel C'). As a control, an N-terminally
307 truncated version of pOv8.25 (TOv8.25CDS-EYFP; starting at M51) was analyzed in the
308 same manner but did not co-localize with a particular subcellular structure (panels G,I).
309 Thus, an intact pOv8.25 was required to achieve the particular subcellular localization of
310 the fusion protein.
311 Moreover, the results shown in Fig. 10 indicated that pOv8.25-EYFP indeed co-
312 localized predominantly but not exclusively with the mitochondria. At 48 hrs a significant
313 co-localization with the ER membranes was also noted. In contrast, co-localization with
314 Golgi membranes was not detected under the present experimental conditions.

315 **The pOv8.25-EYFP fusion protein induces cell death in a bovine lymphocyte cell line**

316 The previous observations that cells expressing the newly detected protein showed
317 quite often an enlarged nucleus and that the yields of pOv8.25-EYFP protein always
318 seemed to be low obtained a new significance, when co-localization of the protein with
319 the mitochondrial membranes was observed. Accordingly, we hypothesized that
320 pOv8.25 may induce cell death. To test this hypothesis and to see, whether or not this
321 was the case in bovine lymphocytes, we made use of Tp951-f53, a previously
322 characterized *Theileria parva*-transformed Bovine cell line (30), which was triple positive
323 for CD4, CD25, and FoxP3, thus, carrying the markers of regulatory T-cells (Tregs).
324 Accordingly, Tp951-f53 cells were non-transduced or transduced with either Ov8.25L-
325 EYFP or Ov8.25cds-EYFP or, as a negative control, with a GFP construct. After 24 hrs,
326 the cells were stained with annexin-V (A-V) and propidium iodide (P.I.) and successfully

transduced cells were gated according to their fluorescence before analysis their status concerning A-V and P.I. by FACS. The results, are shown in Fig. 11. Non-transduced cells (Fig. 11A) were used to set the cut-off for fluorescing cells in gate C. Although the transfection rate was not high, fluorescent cells could be detected in panels B, C, and D. These fluorescent cells in gate C were analyzed for their A-V and P.I. status. As shown in panel B, 45% of the GFP-transduced cells were double negative for A-V and P.I., whereas 52% were double-positive. However, upon transduction with the Ov8.25 constructs, the ratio of double positive cells amounted to nearly 99%, with only few cells remaining viable.

We concluded from these observations that indeed pOv8.25 may induce cell death, even in an immortalized bovine lymphocyte cell line.

Investigating into the pathway of pOv8.25-mediated cell death

In order to address the pathway of pOv8.25-mediated cell death, Vero 2-2 cells were transfected with Ov8.25-EYFP constructs or, as controls, with the N-terminally truncated Ov8.25-EYFP constructs or with EYFP alone. Replicate cultures were harvested at 48 and 72 hrs post transfection and double-stained with annexin V (AV) and propidium iodide (PI) prior to analysis by FACS. The results, showing EYFP-gated cells, are presented in Fig. 12.

Upon transfection, cell viability decreased over time, even with the three control constructs (EYFP, TOv8.25_EYFP, TOv8.25CDS_EYFP). Yet, at 48 hrs post transfection with these controls, 67 to 70% of the cells remained viable. In contrast, only 41 to 43% of the cells transfected with intact Ov8.25-EYFP remained viable. At 72 hrs the viable cells were further reduced with 45-55% remaining viable upon transfection with the control constructs but only 20% cells surviving upon transfection with intact Ov8.25. Moreover, the proportion of Annexin V-positive but PI-negative cells at 48 hrs post transfection amounted to approximately 40% with cells transfected with intact Ov8.25, whereas only around 20% of the controls were positive for this marker of apoptosis. At 72 hrs post transfection, the proportion of Annexin V-positive but PI-negative cells remained almost stable with the controls (20-30%), while it actually decreased with the cells transfected with intact Ov8.25 (26-29%). In contrast, the

proportion of double-positive cells was two to three-fold higher in cells transfected with intact Ov8.25 (48-50%) compared to the controls (11-21%).

Thus, cells transfected with intact Ov8.25 went into apoptosis (AV-positive/PI-negative) at around 48 hrs post transfection and showed predominantly signs of late apoptosis (AV and PI-double positive) at 72 hrs post transfection.

pOv8.25-mediated cell death inhibited by caspase inhibitors

Having established that pOv8.25 targeted mitochondria and that successfully transfected cells showed consecutively signs of early and late apoptosis, it was of interest to test, whether or not this effect could be inhibited by caspase inhibitors. Similar to the previous experiment, Vero 2-2 cells were transfected with Ov8.25-EYFP constructs or, as a negative control, with EYFP alone. Replicate cultures were incubated either in the presence or the absence of a pan-caspase inhibitor, Z-VAD-FMK. Replicate cell cultures were harvested at 48 and 72 hrs post transfection and double-stained with AV and PI prior to analysis by FACS. The experiment was repeated five times and, despite of varying transfection efficiencies (Fig. 13A), always with the same outcome, namely increased cell death in the presence of the Ov8.25 protein (Fig. 13 B through E). Both at 48 and 72 hrs, the proportion of live cells (AV/PI-double negative) among Ov8.25-transfected cells was significantly reduced compared to EYFP-transfected cells (Fig. 13B,C). However, in the presence of caspase inhibitors, the viability of Ov8.25- and EYFP-transfected cells was not significantly different. Interestingly, the predominant phenotype of non-viable cells at 48 hrs differed from that at 72 hrs. At 48 hrs, early apoptotic cells (AV-positive/PI-negative) were significantly increased among Ov8.25-transfected cells without caspase inhibitors compared to either EYFP-transfected cells, independent of caspase inhibitors, or else Ov8.25-transfected cells in the presence of caspase inhibitors (Fig. 13D). However, at 72 hrs, late apoptotic cells (AV/PI double positive) made a similar, highly significant difference between Ov8.25-transfected cells without and Ov8.25-transfected cells with caspase inhibitors or EYFP-transfected cells, independent of presence or absence of inhibitors (Fig. 13E). A general loss of viable cells observed at 72 hrs compared to 48 hrs post transfection was attributed to stressing the cells due to the transfection protocol.

Thus, the cell death induced following transient expression of pOv8.25 was indeed due to caspase-dependent cell death.

Detection of pOv8.25 in brain-infiltrating lymphocytes of cattle with MCF.

Based on the previous results, it was of interest to test, whether or not pOv8.25 was detectable in pathognomonic lesions of cattle with MCF. Due to the scarcity of fresh cases, historic samples of cattle with histologically confirmed encephalitis were used for this purpose. Indeed, immunohistological signals of pOv8.25 were detected among infiltrating lymphocytes in brain sections of two of those cases (Fig. 14A,B). The same signals remained undetectable upon prior saturation of the antiserum with the immunizing peptide. Although they comprised histologically similar brain lesions, the other two cases, which had previously deemed OvHV2-negative by PCR, did not show any detectable pOv8.25 (Fig. 14C,D). Thus, as a proof of principle, pOv8.25 could be detected within typical MCF lesions.

Discussion

In this communication, we describe a previously overlooked gene of OvHV-2, which was only noticed because of its abundant expression in animals with MCF (21). In lymphatic tissues of such animals as well as in persistently infected cell cultures (LGL) and upon transient expression in transfected or transduced cells, this newly identified gene is expressed as a double spliced mRNA. This gene, termed Ov8.25 due to its location within the OvHV-2 genome, encodes for a protein (pOv8.25) that targets the mitochondria in a manner to inducing apoptosis and necrosis.

There are several distinct viruses that cause clinically and histopathologically very similar illnesses, all of them believed to represent the same disease, MCF. These viruses are genetically similar among each other and taxonomically grouped together in the genus *Macavirus* of the subfamily *Gammaherpesvirinae*, yet each one of them has also a number of specific genes that discriminate these viruses as a group from the other genera of the gammaherpesviruses and at the individual level each member from the other members of the genus (1, 21, 31). These genes are named in relation to the virus they belong to, for example A1 through A10 in the case of AlHV-1 or, respectively,

Ov2 through Ov10 in the case of OvHV-2. The nomenclature stems from the sequence of AlHV-1, which had been published first and is, therefore, recognized as the prototype (32). The numbering was from left to right on the original sequence. Later on, additional members of these specific genes were detected, which led to the introduction of "0.5" nomenclature, depending on the relative position of the newly detected gene among the original enumeration (8, 33, 34). For example, A4.5 was designated as such for its position in between of A4 and A5. The Ov-nomenclature was then adopted to use the same enumeration for potential orthologues to particular A-genes in OvHV-2 (33, 34). For example, a potential orthologue to A1 was not detected in the OvHV-2 sequence. Consequently, OvHV-2 has no Ov1. However, the first OvHV-2-specific gene was termed Ov2 for its similarity to A2. Moreover, the OvHV-2 genome has an additional specific gene in between of Ov2 and Ov3, which was designated Ov2.5 (35). Based on these considerations and the map location of the newly detected gene in between of Ov8 or, more narrowly ORF69, and Ov8.5, we named it Ov8.25. Interestingly, the Ov8.25 gene is not only conserved among various OvHV-2 isolates (Fig. 2) but has also a positional homologue in AlHV-1, termed expressed region 16 (ER16), which is highly transcribed during experimental MCF (20). Of note, a small open reading frame within ER16 has the capacity to encode for an 11.3 kDa hydrophobic protein with two transmembrane regions, which shares a PVQC-motif near its C-terminus with our newly detected pOv8.25. Thus, this genomic locus and its protein may be one of the important players in the pathogenesis of MCF, which is, despite of recent progress, still not fully understood (8, 21, 36-39). However, it remains to be confirmed that an orthologue to this gene exists also in other Macaviruses.

Based on recent evidence, it can be assumed that the main portal of entry of OvHV-2 into cattle is by the respiratory route and relies on at least a few rounds of lytic replication of OvHV-2 in deep lung tissue (23, 40). Later on, OvHV-2 -- as well as AlHV-1 -- is disseminated systemically in the infected organism, affecting different types of peripheral blood mononuclear cells (PBMC), particularly lymphocytes, but remaining now in a predominantly latent form of the infection as evidenced by viral gene expression assays (20, 21, 41). With the onset of clinical symptoms, a loss of overall lymphocyte counts goes along with the histological picture of non-purulent inflammation,

apoptosis and necrosis not only of lymphoid tissue but also of blood vessels in various organs due to accumulation of activated T-cells (8). Our finding that pOv8.25 targets the mitochondria to induce apoptosis and necrosis fits in very well with these histopathological findings in animals with MCF. The detection of pOv8.25 in infiltrating lymphocytes within typical MCF lesions (Fig. 14) supports this notion as a proof of principle.

In the light of our present findings, we speculate that particularly the pronecrotic property of pOv8.25 (Fig. 12) might contribute to the severity and perpetuation of the disease: expression of pOv8.25 in various cell types, thus, causing their apoptosis and necrosis will facilitate extravasation of PBMC and, since they are also infected and expressing Ov8.25, generation of necrotic foci around such vessels might eventually attract an inflammatory reaction. In this context, it was important to show that a truncated form of pOv8.25 had lost its ability to target the mitochondria (Fig. 9) and, consequently failed in its pronecrotic facility (Fig. 12). Moreover, we were able to demonstrate that the killing activity of pOv8.25 does extend even to seemingly immortalized bovine lymphocytes with a Treg phenotype (Fig. 11), whose regulating activity would be much needed to curb the destructive effects of activated killer cells. Our results also shed a new light on the old debate about the roles of the latent or proliferative forms of the virus throughout the disease. In AlHV-1 it has been firmly established that an intact ORF73, encoding the major latency associated nuclear antigen (LANA), is essential for the development of WA-MCF (20). It has not been possible to establish the same for OvHV-2 and SA-MCF because, due to its inability to replicate in conventional cell cultures, there has not yet been any success in genetically modifying OvHV-2. However, a less strictly regulated gene expression pattern during MCF has been observed with OvHV-2 as compared to AlHV-1 (reviewed in (1)). Indeed, the transcripts of several lytic OvHV-2 genes have consistently been observed in MCF lesions, among others, the transcript for the major capsid protein, which is encoded by ORF25 (23). In the rabbit model, the lytic proteins encoded by ORF43 and ORF67 could directly be detected within MCF lesions by using specific antisera (22). However, these observations are contrasted by the absence of demonstrable viral particles in the lesions of clinically affected animals (1, 42, 43).

Unresolved issues. (1) From our Westernblots (Fig. 7), we gained the suspicion that pOv8.25 either interacts covalently with at least one host protein or is able to form homopolymers. It was beyond the scope of this work to address this issue further but it would be highly interesting to know the putative interaction partners of pOv8.25. (2) It is well accepted that viruses do not carry genes for no purpose. Therefore, we have to assume that the Ov8.25 locus, its protein as well as potentially its introns play a role in the natural life cycle of OvHV-2 among sheep. Understanding this role would be very helpful for considering what goes wrong to cause MCF in the indicator host. It might be possible to address this issue in the future, provided that a BAC-cloned OvHV-2 would be available. (3) As we recognize that Ov8.25 seems to be important enough for OvHV-2 to keep it conserved among vastly different isolates (Scotch, American, Swiss; Fig. 2), we have to assume as well that it is expressed throughout replication and/or latency in sheep. Yet, its true function remains obscure.

Conclusions. We have characterized a previously overlooked genetic locus in OvHV-2, which is conserved among viruses causing Malignant catarrhal fever and highly transcribed throughout disease. In OvHV-2, the transcript is double spliced, giving rise to a short protein with two transmembrane regions, which targets the mitochondria, causing apoptosis and necrosis in various cell types and which can be detected in affected brain tissue. An N-terminal truncation of this protein abrogates its proapoptotic properties. With Ov8.25 mRNA (21) and its encoded protein with its newly reported properties present in MCF lesions, we may now begin to understand some destructive aspects of the disease phenotype. We even speculate that pOv8.25 might represent an important trigger for the development of MCF.

Materials and Methods

Ethic statement and animals.

The study did not require anesthesia, euthanasia, or any kind of animal sacrifice.

Samples from animals with MCF.

Lymphocytes from a Swiss cow with OvHV-2 associated MCF were kindly provided by Dr. Marco Franchini (University of Zurich, Switzerland).

OvHV-2-infected large granular lymphocytes (LGLs).

Persistently OvHV-2-positive LGL were kindly provided by Dr. George Russel, Moredun Research Institute, Edinburgh, Scotland.

RLM-RACE and cloning

RNA Ligase Mediated Rapid Amplification of cDNA Ends (RLM-RACE)

Total RNA was extracted from OvHV-2-positive materials and 2 to 5 µg were used for RLM-RACE (Ambion FirstChoice RLM-RACE Kit from Thermo Fisher Scientific). The protocol followed essentially the supplier's recommendations. Briefly, for 5' RACE, RACE adapters were ligated to the targeted RNA templates before reverse transcription was initiated using a sequence-specific reverse primer. The cDNA was then used for nested PCR. For 3' RACE, reverse transcription was started from the 3' RACE adapter, whereas the consecutive nested PCR needed a pair of sequence-specific forward primers, bracketing the targeted sequence with a pair of reverse primers provided in the kit. Eventually, these PCRs provided enough amplification product for cloning and sequencing. The primers used are listed in Table. 1.

Cloning of the Ov8.25 locus into pEGFP N3

The newly determined Ov8.25 locus was amplified by bracketing PCR primers (Table. 2), which were supplemented with specific restriction enzyme digestion sites for later orientation-dependent subcloning. The ensuing 750 bp PCR product was initially cloned into the TOPO TA vector. After verifying its desired sequence, the desired fragment was excised from the TOPO vector by double digestion with NheI and EagI, whereas the pEGFP-vector was opened by NheI and NotI digestion. After agarose gel electrophoresis, the desired fragments were cut out, pooled, and liquefied for in-gel-ligation, using 1 µl of the vector (gel), 4 µl of the DNA fragment/insert (gel), 1 µl T4 DNA ligase, 2.5 µl T4 DNA buffer, and nuclease-free H_2O to give a final volume of 26 µl.

Sequencing of the ensuing cloned construct confirmed that the Ov8.25 locus was now in the pEGFP N3 vector and under the control of the cmvIE promoter.

Synthetic constructs

Synthetic DNA sequences were obtained from GenScript (Piscataway, NJ, U.S.A.). The Gateway Technology (Invitrogen/Thermo Fisher Scientific) was used to transfer the synthetic constructs into pHSV-amplicon vectors, whose design has been described (27). A summary of the constructs is provided in Table. 3.

Cell culture

Vero 2-2 cells are derived from African green monkey Vero kidney epithelial cell line by incorporating a plasmid containing the IE2 (ICP27) gene and promoter into the genome. Vero 2-2 cells were cultured in DMEM (Life Technologies) containing 10% heat inactivated fetal bovine serum FCS, geneticin (500 µg/ml). Cells were cultured at 37°C in a humidified atmosphere containing 5% CO_2.

HEK 293T cells were obtained from ATCC and are human embryonic kidney cells, which contain Adeno and SV-40 viral DNA sequences and which are particularly suitable for transient expression assays. These cells were also kept in DMEM, propagated with FCS and kept in 5% CO_2.

Theileria-Parva (T.p) transformed bovine T-lymphocytes (**generously** gifted by late Prof. Dobbeleare, Institute of molecular parasitology, University of Bern) were cultured in RPMI 10% heat inactivated fetal bovine serum (FBS) (10500-064, GIBCO), 1% penicillin/streptomycin and 0.001% ß-Mercaptoethanol (60242, SIGMA-ALDRICH). Cells were cultured at 37°C in a humidified atmosphere containing 5% CO2. **Tp951-f53**: Cell line clone of PBMCs of animal 951 which were infected with T. p. Marikebuni, (CTVM, stabilate 72) of genotype F53 and cloned by limiting dilution. **Tp951-f31**. Cell line clone of PBMCs of animal 951 which were infected with T. p. Marikebuni, (CTVM, stabilate 72) of genotype F31 and cloned by limiting dilution.

Transient expression

For transient expression, cloned DNA was transfected using Lipofectamin LTX into either HEK 293T or Vero 2-2 cells. 48 h after transfection, total RNA was extracted using the RNeasy mini kit (QIAGEN), Hombrechtikon, Switzerland. The extracted RNA

was reverse transcribed using the reverse transcription protocol of Promega. The phusion high- fidelity DNA polymerase (FINNZYMES, Thermo Fisher Scientific, Reinach, Switzerland) was used to amplify the cDNA by PCR, using primers (listed in Tab. 2), which bracketed the introns of interest. The amplified PCR products were then run on 2% agarose gel (NEEO ultra quality agarose, ROTH AG, Arlesheim, Switzerland).

Polyacrylamide gel electrophoresis and Western transfer

Post 24 h of transfection, the cells were washed once with PBS before 160 µl of IP buffer (1% Triton-X100, 20 m M Tris, 50 mM Nacl, 50 mM NaF, 150 mM $Na_4P_2O_7$, 10 mM EDTA) was added. The cells were then scrapped off and transferred into a 1.5 ml Eppendorf tube to be incubated on ice for 15 min. The lysate was then centrifuged in an Eppendorf centrifuge for 15 min at 13000 rpm and at 4°C. The soluble (supernatant) and insoluble (cell pellet) fractions were separated in two tubes. The cell pellet was re-suspended in 84 µl of PBS and mixed with 16 µl of 6x Lämmli buffer whereas 33 µl of 6x Lämmli buffer was added to the supernatant and boiled for 10 min at 95°C. The protein lysates were run in 15% of polyacrylamide gels at 100 V for 2 hrs before being transferred onto PVDF membranes (BIO-RAD) at 100 V for 1.5 hrs.

Fluorescence microscopy and confocal microscopy

Separate dishes of transfected cells were incubated at 37°C for 6, 24 or 48 h, respectively. In order to stain mitochondria, after each incubation time, cells were washed 1X with PBS before mitotracker deep red (Invitrogen) diluted in culture medium (final concentration of 300 µM) was added to the respective wells and incubated for 15 min at 37°C. In order to stain ER and golgi apparatus of transfected cells, cells were fixed with 4% PFA for 25 min followed by permeabilization with 0.1% Triton-X100 for 2 min. Subsequently, cells were stained with ConA (20 µg/ml) and WGA (5 µg/ml) for 25 min at RT. Stained cells were washed once with PBS and once with H_2O. Finally, a drop of Roti-Mount FluorCare DAPI was overlaid and the cells were covered with a glass coverslip before being analyzed using confocal microscope at respective wavelengths, EYFP: 488 nm; ConA: 594 nm; WGA: 594 nm; Mitotracker deep red: 633 nm. Images

were taken which were analyzed using Imaris software. To quantify the amount of co-localization, a previously established method (Manders' overlap coefficient) was used (28).

Fluorescent stains

The following fluorescent stains were used: Roti-Mount FluorCare DAPI (Carl Roth GmbH, Karlsruhe, Germany), Mitotracker deep red (633 nm; Invitrogen, Carlsbad, CA, USA), ConA-Alexa-594, WGA-Alexa-594, FITC annexin V (AV) (Abcam, Cambridge, UK) and propidium iodide (P.I.) (Sigma-Aldrich, St. Louis, MI, USA).

Annexin/PI staining

Vero 2-2 cells were seeded in 6 wells plate at the confluency of 90%. Next day, cells were either left non-transfected or transfected with respective plasmids. After either 48 h or 72 h, cells were harvested and washed once with PBS. Working dilution (100 µg/ml) of Propidium iodide (PI) (Sigma-Aldrich Chemie GmbH, Buchs SG, Switzerland) was prepared. Then 2 µl of FITC annexin V (Abcam, Cambridge, UK) and 1 µl of PI (from working dilution) was added to 100 µl of 1X annexin-binding buffer. Washed cells were re-suspended in 100 µl of 1X annexin-binding buffer and incubated for 15 min in dark. Then the cells were filtered through polystyrene round bottom FACS tube with cell-strainer cap (BD Falcon) and data was acquired using Flow cytometry. Three different channels were used. FL1: EYFP, FL4: PI and FL6: Cy5. The acquired data were analyzed using Kaluza analysis (Beckman Coulter).

Purified antibodies against Ov8.25 protein

A rabbit anti-peptide serum was commercially produced and purified by GenicBio Limited, Sanghai, China. The immunizing synthetic peptide (KKKDKKRDEDEDEDEDE-C) was conjugated to KLH. Specific antibodies were purified from the resulting antiserum using peptide-specific affinity.

Pre-immune serum (2 ml), purified antibodies (4 mg) as well as 10 mg of unconjugated peptide were provided in lyophilized form.

Immunohistochemistry

Due to the scarcity of the disease, tissues from fresh MCF cases were unavailable. As an alternative, we took advantage of an existing collection of formaldehyde-fixed, paraffin embedded brain tissues from suspected BSE cases, which, though, had been deemed BSE-negative but whose pathological diagnosis was encephalitis, probably due to viral origin. One of those cases (#44282 from 2010; thalamus) had been deemed OvHV2-positive by PCR, whereas two other cases (# 33181 from 2001; brain stem and # 26731 from 1998; brain stem) had been deemed negative for OvHV-2. In the fourth case (#51194 from 2018; brain stem), listeriosis had been diagnosed but OvHV-2 was not formally excluded on fresh tissue. The brain tissues were cut into 3µm sections. After antigen retrieval by boiling the samples for 20 minutes in a microwave in the presence of the antigen retrieval buffer (LSAB™, DAKO), the sections were incubated over-night at 4°C with either the purified Rabbit-anti-pOv8.25 serum or else with peptide-saturated antiserum. Subsequently, the reactions were made visible using a streptavidin–biotin-complex method (LSAB™, DAKO) and AEC as chromogen.

Acknowledgments

This work was financed by a grant from the Swiss National Science Foundation to M.A. (SNF 310030-130456), from a private donation of the late Robert Wyler to M.A. (F-52601-10-01), as well as by general funds allocated to M.A. by the University of Zurich.

References

1. Li H, Cunha CW, Taus NS, Knowles DP. 2014. Malignant catarrhal fever: inching toward understanding. Annu Rev Anim Biosci 2:209-33.
2. Bedelian C, Nkedianye D, Herrero M. 2007. Maasai perception of the impact and incidence of malignant catarrhal fever (MCF) in southern Kenya. Prev Vet Med 78:296-316.
3. Whitaker KA, Wessels ME, Campbell I, Russell GC. 2007. Outbreak of wildebeest-associated malignant catarrhal fever in Ankole cattle. Vet Rec 161:692-5.
4. Meteyer CU, Gonzales BJ, Heuschele WP, Howard EB. 1989. Epidemiologic and pathologic aspects of an epizootic of malignant catarrhal fever in exotic hoofstock. J Wildl Dis 25:280-6.
5. Castro AE, Ramsay EC, Dotson JF, Schramke ML, Kocan AA, Whitenack DL. 1984. Characteristics of the herpesvirus of malignant catarrhal fever isolated from captive wildebeest calves. Am J Vet Res 45:409-15.

6. Muller-Doblies UU, Egli J, Li H, Braun U, Ackermann M. 2001. [Malignant catarrhal fever in Switzerland. 1.Epidemiology]. Schweiz Arch Tierheilkd 143:173-83.
7. Li H, Cunha CW, Abbitt B, deMaar TW, Lenz SD, Hayes JR, Taus NS. 2013. Goats are a potential reservoir for the herpesvirus (MCFV-WTD), causing malignant catarrhal fever in deer. J Zoo Wildl Med 44:484-6.
8. Russell GC, Stewart JP, Haig DM. 2009. Malignant catarrhal fever: a review. Vet J 179:324-35.
9. Ackermann M. 2006. Pathogenesis of gammaherpesvirus infections. Vet Microbiol 113:211-22.
10. Reid HW, Buxton D, Berrie E, Pow I, Finlayson J. 1984. Malignant catarrhal fever. Vet Rec 114:581-3.
11. Albini S, Zimmermann W, Neff F, Ehlers B, Hani H, Li H, Hussy D, Casura C, Engels M, Ackermann M. 2003. [Porcine malignant catarrhal fever: diagnostic findings and first detection of the pathogenic agent in diseased swine in Switzerland]. Schweiz Arch Tierheilkd 145:61-8.
12. Ackermann M. 2005. [Virus in sheep's skin]. Schweiz Arch Tierheilkd 147:155-64.
13. Sood R, Hemadri D, Bhatia S. 2013. Sheep associated malignant catarrhal fever: an emerging disease of bovids in India. Indian J Virol 24:321-31.
14. Stahel AB, Baggenstos R, Engels M, Friess M, Ackermann M. 2013. Two Different Macaviruses, ovine herpesvirus-2 and caprine herpesvirus-2, behave differently in water buffaloes than in cattle or in their respective reservoir species. PLoS One 8:e83695.
15. Lapp S, Forster C, Kummrow M, Wohlsein P, Haist V. 2015. Malignant catarrhal fever in a Vietnamese pot-bellied pig. A potential threat to pigs in mixed-species exhibits? Tierarztl Prax Ausg G Grosstiere Nutztiere 43:165-8.
16. Haigh JC, Mackintosh C, Griffin F. 2002. Viral, parasitic and prion diseases of farmed deer and bison. Rev Sci Tech 21:219-48.
17. O'Toole D, Li H, Sourk C, Montgomery DL, Crawford TB. 2002. Malignant catarrhal fever in a bison (Bison bison) feedlot, 1993-2000. J Vet Diagn Invest 14:183-93.
18. Muller-Doblies UU, Egli J, Hauser B, Li H, Strasser M, Ehrensperger F, Braun U, Ackermann M. 2001. [Malignant catarrhal fever in Switzerland: 2. Evaluation of the diagnosis]. Schweiz Arch Tierheilkd 143:581-91.
19. O'Toole D, Li H. 2014. The pathology of malignant catarrhal fever, with an emphasis on ovine herpesvirus 2. Vet Pathol 51:437-52.
20. Palmeira L, Sorel O, Van Campe W, Boudry C, Roels S, Myster F, Reschner A, Coulie PG, Kerkhofs P, Vanderplasschen A, Dewals BG. 2013. An essential role for gamma-herpesvirus latency-associated nuclear antigen homolog in an acute lymphoproliferative disease of cattle. Proc Natl Acad Sci U S A 110:E1933-42.
21. Meier-Trummer CS, Rehrauer H, Franchini M, Patrignani A, Wagner U, Ackermann M. 2009. Malignant catarrhal fever of cattle is associated with low abundance of IL-2 transcript and a predominantly latent profile of ovine herpesvirus 2 gene expression. PLoS One 4:e6265.
22. Meier-Trummer CS, Tobler K, Hilbe M, Stewart JP, Hart J, Campbell I, Haig DM, Glauser DL, Ehrensperger F, Ackermann M. 2009. Ovine herpesvirus 2 structural proteins in epithelial cells and M-cells of the appendix in rabbits with malignant catarrhal fever. Vet Microbiol 137:235-42.

23. Nelson DD, Taus NS, Schneider DA, Cunha CW, Davis WC, Brown WC, Li H, O'Toole D, Oaks JL. 2013. Fibroblasts express OvHV-2 capsid protein in vasculitis lesions of American bison (Bison bison) with experimental sheep-associated malignant catarrhal fever. Vet Microbiol 166:486-92.
24. Mushi EZ, Rurangirwa FR. 1981. Epidemiology of bovine malignant catarrhal fevers, a review. Vet Res Commun 5:127-42.
25. Hussy D, Stauber N, Leutenegger CM, Rieder S, Ackermann M. 2001. Quantitative fluorogenic PCR assay for measuring ovine herpesvirus 2 replication in sheep. Clin Diagn Lab Immunol 8:123-8.
26. Li H, Taus NS, Lewis GS, Kim O, Traul DL, Crawford TB. 2004. Shedding of ovine herpesvirus 2 in sheep nasal secretions: the predominant mode for transmission. J Clin Microbiol 42:5558-64.
27. Meier AF, Laimbacher AS, Ackermann M. 2016. Polycistronic Herpesvirus Amplicon Vectors for Veterinary Vaccine Development. Methods in molecular biology (Clifton, N J) 1349:201-24.
28. Dunn KW, Kamocka MM, McDonald JH. 2011. A practical guide to evaluating colocalization in biological microscopy. Am J Physiol Cell Physiol 300:C723-42.
29. Omasits U, Ahrens CH, Muller S, Wollscheid B. 2014. Protter: interactive protein feature visualization and integration with experimental proteomic data. Bioinformatics 30:884-6.
30. Dobbelaere DA, Coquerelle TM, Roditi IJ, Eichhorn M, Williams RO. 1988. Theileria parva infection induces autocrine growth of bovine lymphocytes. Proc Natl Acad Sci U S A 85:4730-4.
31. Davison AJ, Eberle R, Ehlers B, Hayward GS, McGeoch DJ, Minson AC, Pellett PE, Roizman B, Studdert MJ, Thiry E. 2009. The order Herpesvirales. Arch Virol 154:171-7.
32. Ensser A, Pflanz R, Fleckenstein B. 1997. Primary structure of the alcelaphine herpesvirus 1 genome. J Virol 71:6517-25.
33. Hart J, Ackermann M, Jayawardane G, Russell G, Haig DM, Reid H, Stewart JP. 2007. Complete sequence and analysis of the ovine herpesvirus 2 genome. J Gen Virol 88:28-39.
34. Taus NS, Herndon DR, Traul DL, Stewart JP, Ackermann M, Li H, Knowles DP, Lewis GS, Brayton KA. 2007. Comparison of ovine herpesvirus 2 genomes isolated from domestic sheep (Ovis aries) and a clinically affected cow (Bos bovis). J Gen Virol 88:40-5.
35. Jayawardane G, Russell GC, Thomson J, Deane D, Cox H, Gatherer D, Ackermann M, Haig DM, Stewart JP. 2008. A captured viral interleukin 10 gene with cellular exon structure. J Gen Virol 89:2447-55.
36. Li H, Cunha CW, Taus NS. 2011. Malignant catarrhal fever: understanding molecular diagnostics in context of epidemiology. Int J Mol Sci 12:6881-93.
37. Sorel O, Chen T, Myster F, Javaux J, Vanderplasschen A, Dewals BG. 2017. Macavirus latency-associated protein evades immune detection through regulation of protein synthesis in cis depending upon its glycin/glutamate-rich domain. PLoS Pathog 13:e1006691.
38. Nightingale K, Dry I, Hopkins J, Dalziel R. 2019. Regulation of Ov2 by virus encoded microRNAs. Vet Res Commun doi:10.1007/s11259-019-09749-9.

744 39. Dry I, Nightingale K, Ferguson J, Hopkins J, Dalziel R. 2019. Ov2 is a modulator of
745 OvHV-2 RTA mediated gene expression. Vet Res Commun doi:10.1007/s11259-019-
746 09748-w.
747 40. Bartley K, Deane D, Percival A, Dry IR, Grant DM, Inglis NF, McLean K, Manson ED,
748 Imrie LH, Haig DM, Lankester F, Russell GC. 2014. Identification of immuno-reactive
749 capsid proteins of malignant catarrhal fever viruses. Vet Microbiol 173:17-26.
750 41. Dewals B, Boudry C, Farnir F, Drion PV, Vanderplasschen A. 2008. Malignant catarrhal
751 fever induced by alcelaphine herpesvirus 1 is associated with proliferation of CD8+ T
752 cells supporting a latent infection. PLoS One 3:e1627.
753 42. Bridgen A, Munro R, Reid HW. 1992. The detection of Alcelaphine herpesvirus-1 DNA
754 by in situ hybridization of tissues from rabbits affected with malignant catarrhal fever. J
755 Comp Pathol 106:351-9.
756 43. Rossiter PB. 1980. A lack of readily demonstrable virus antigens in the tissues of rabbits
757 and cattle infected with malignant catarrhal fever virus. Br Vet J 136:478-83.
758

759 ## Figure legends

760 **Fig. 1. RACE experiments to determine the ends of the novel transcript**. 1%
761 agarose gel showing RLM-RACE PCR products obtained from RNA of an MCF-affected
762 cow. Lane 1: 3'RACE after first amplification. Lane 2: 3'RACE after nested amplification.
763 Lane 3: 5'RACE after first amplification. Lane 4: 5'RACE after nested amplification.
764 Lane 5: 1 kb DNA marker

765 **Fig. 2. Conservation of Ov8.25 locus and splicing.** Sequence alignment of the novel
766 transcripts found in the LGLs (RNA_lgl) and in lymphocytes of a cow with MCF
767 (RNA_cow) against published OvHV-2 genomic sequences. The predicted translation
768 initiation codon (ATG) is highlighted in bold letters. The two predicted introns in the
769 processed transcripts are highlighted in red. The asterisks indicate identical nucleotides
770 in all four sequences. The internal gene-specific primers used for RACE are highlighted
771 in blue. The sequences of the forward primers and the complementary sequences of the
772 reverse primers, respectively, for cloning into the pEGFP N3 expression vector are
773 highlighted in green.

774 **Fig. 3. The Ov8.25 transcript is smaller than its DNA template**. Amplified PCR
775 products on a 2.5% agarose gel with the DNA size marker in the lanes 1 and 6. The
776 lanes 2, 3, and 4 show the PCR products obtained from decreasing amounts of cDNA

777 template (3.2 µl, 1.9 µl, 1.5 µl cDNA template, respectively). For lane 5, the transfecting
778 DNA construct was used as template.
779 **Fig. 4. Compartmentalized localization of pOv8.25-EYFP fusion protein**. Vero 2-2
780 cells under the fluorescence microscope at 24 hrs after transfection with either
781 pHSV_EGFP (A) or pHSV_Ov8.25-EYFP (B).
782 **Fig. 5. Conserved splicing of Ov8.25 transcripts**. Reverse transcription PCR using
783 RNA template, harvested at 24 hrs post transfection of Vero 2-2 cells with synthetic
784 Ov8.25 amplicon constructs.
785 Each construct is represented in three consecutive lanes and each triplet is labeled
786 beneath the lanes with the designation of the construct. The first lane (lanes 2, 5, 8, 11,
787 15) in each triplet represents a control using plasmid DNA as template. For the second
788 lane (lanes 3, 6, 9, 12, 16), reverse transcribed RNA extract had been used as PCR
789 template. For the third lane (lanes 4, 7, 10, 13, 17), RNA extract was PCR amplified
790 without prior reverse transcriptase treatment. Lanes 1 and 14: 100 bp DNA size ladder,
791 with a strong 500 bp band.
792 **Fig. 6. Predicted structure of pOv8.25**, including M1, M51 (blue), two transmembrane
793 domains, and predicted antibody epitope (yellow), which was used to generate a rabbit
794 antiserum against pOv8.25.
795 (Figure generated using protter (29))
796 **Fig. 7. Apparent mobility and solubility of pOv8.25.** Western immunoblot of
797 transfected Vero 2-2 cells. A, B, C) Labeled with anti-GFP monoclonal antibody. (A')
798 Replicate blot, labeled with anti-actin monoclonal antibody. (B', C') Blots from B and C
799 re-stained with anti-tubulin monoclonal antibody.
800 Panels A, A') Lane M: molecular weight marker. Blue band labeled on the left: 35 kDa.
801 Lanes 1-4: transfected cell extracts, harvested at 24 hrs. Lane 1: EYFP-amplicon; lane
802 2: codon-optimized, intronless Ov8.25 coding sequence with C-terminal EYFP; lane 3:
803 codon-optimized Ov8.25 locus with C-terminal EYFP. Lane 4: untransfected cell extract.
804 Panels B, B', C, C') Harvested cells were suspended in IP buffer containing 1% Triton
805 X100, before soluble and insoluble extracts were separated by centrifugation.
806 Both fractions were separately taken up in SDS buffer a separated by PAGE. Finally,
807 Western transfers were stained using monoclonal antibodies. Lanes 1: non-transfected

Vero cells. Lanes 2-6: transfected Vero cells. 2: transfected with EYFP; 3: codon-optimized Ov8.25 locus with C-terminal EYFP; 4: codon-optimized, intronless Ov8.25 coding sequence with C-terminal EYFP; 5: 5'-truncated codon-optimized Ov8.25 locus with C-terminal EYFP; 6: 5'-truncated codon-optimized, intronless Ov8.25 coding sequence with C-terminal EYFP.

Red arrow indicating 38.7 kDa, the predicted mobility of pOv8.25-EYFP fusion protein.

Fig. 8. Identification of pOv8.25 by anti-peptide serum. Western immunoblots of insoluble cell extracts. Panel A) Labeled with rabbit anti pOv8.25 serum. Panel B) Labeled with anti-GFP monoclonal antibody. C) Labelled with antibody that was primarily saturated with immunizing peptide.

Lane M: Page ruler plus, molecular weight marker. MWs indicated on the left. Lane 1: non-tranfected Vero cells; Lane 2: transfected with EYFP; Lane 3: transfected with codon-optimized Ov8.25 locus with C-terminal EYFP; Lane 4: transfected with codon-optimized, intronless Ov8.25 coding sequence C-terminal EYFP; Lane 5: truncated version of codon-optimized Ov8.25 locus with C-terminal EYFP; Lane 6: truncated version of codon-optimized, intronless Ov8.25 coding sequence C-terminal EYFP.

Red arrows in A) and B) pointing to 38.7 kDa, the predicted mobility of pOv8.25-EYFP fusion protein.

Note: higher molecular bands are recognized by both the rabbit anti-peptide serum and the anti-GFP mcAb. The EYFP band (lane 2) is not recognized by the rabbit anti-peptide serum.

Fig. 9. pOv8.25-EYFP co-localizes with the mitotracker stain. Vero cells were transfected with either Ov8.25-EYFP amplicon DNA (panels A through F) or with a truncated version, which is translated only from the ATG encoding for M51 of the original aa sequence (panels G through I). The cells were fixed at 24 hrs before being stained with DAPI and analyzed by confocal microscopy. Panels A, D and G show yellow fluorescence and DAPI, panels B, E and H show the mitotracker stain and DAPI. Co-localization of EYFP and red fluorescence (mitotracker), indicated by yellow, was addressed in panels C, C', F and I. C' shows a three-dimensional reconstruction of the cell presented in C. The bar in C', F and I represent 10 µm, 20 µm and 30 µm respectively.

Fig. 10. **pOv8.25-EYFP fusion protein co-localizes predominantly with mitochondria**. Vero cells were transfected with Ov8.25-EYFP amplicon DNA and were stained with WGA (panels B, C), red fluorescent Mitotracker (panels E, F) and ConA (panels H, I) in order to test co-localization of pOv8.25-EYFP with individual membrane compartments. (A) Confocal images, supplemented with DAPI stain to show the cell nuclei (blue). Membrane staining is seen in red; yellow fluorescence appears in green; co-localization appears in yellow. The bar represents 30um. (B) Quantitative analysis of the co-localization at 6, 24, and 48 hrs post transfection (Determination of the Mander's coefficient described in Materials and Methods).

Fig. 11. **Synthesis of pOv8.25 is associated with increased cell death in a Bovine Treg-like cell line**. Tp951-f53 cells were left non-transduced (panels A) or were transduced with either EGFP (panels B, B') or Ov8.25 constructs (Ov8.25L-EYFP in panels C, C'; Ov8.25CDS-EYFP in panels D, D'). After 24 hrs, the cells were harvested, double-stained annexin-V and propidium iodide, and gated for fluorescence due to GFP or EYFP.

Panel (A-D) show the total cells where gate C shows the population that has been gated for EYFP expression.

Panel (B'-D') show the AV/PI staining of gated population.

Fig 12: Flow cytometry analysis of AV-CY5/PI double stained and EYFP-gated cells. Vero 2-2 cells were transfected with either V5_EYFP (A,F) or Ov8.25L_EYFP (B,G) or Ov8.25CDS_EYFP (C,H) or TOv8.25_EYFP (D,I) or TOv8.26CDS_EYFP (E,J). Cells harvested at 48 and 72 hrs post transfection were labelled with AV-Cy5 and PI and analyzed by flow cytometry. Cells gated for EYFP-expression are shown. AV negative /PI negative (B--): Viable cells; AV positive /PI negative (B+-): apoptotic cells; AV positive/PI positive (B++): late apoptotic/dead cells.

Fig. 13. Caspase-dependent cell death upon transient expression of Ov8.25. Vero cells were transfected with constructs encoding for Ov8.25-EYFP fusion proteins or EYFP alone and incubated either in the presence or absence of a broad-spectrum caspase inhibitor. The cells were harvested after 48 and 72 hrs, respectively, and stained for AV and PI before being gated for yellow fluorescence. (A) The counts of EYFP-positive, gated cells in each of the five experiments are shown, separately for

cells that had been incubated in the absence (dots) or presence (squares) of the inhibitors as well as for 48 hrs or 72 hrs post transfection. Panels B and C show the medium values and standard deviations from five independent experiments, depicting the proportions of viable (AV/PI-double negative) cells at 48 hrs (B) or 72 hrs (C). Panel D shows the proportions of early apoptotic cells at 48 hrs (AV-positive/PI-negative); Panel E the proportions of late apoptotic cells at 72 hrs (AV/PI double positive). Each column in a panel, representing replicate values from five independent experiments, was compared individually to each other column in the same panel. Significant differences were detected using the unpaired t test (**** indicates a p value of <0.0001).

Fig. 14. Detection of pOv8.25 in MCF-like lesions. Sections of brain tissues from cattle with encephalitis were immune-stained with the rabbit anti-pOv8.25 peptide serum. Positive reactions (Panels A and B) show reddish coloration due to the AEC chromogen in two independent cases, one of which had previously deemed positive for OvHV-2 by PCR. Areas with typical staining are magnified in A' and B'. Panels C and D show samples from two additional unrelated cases, which did not show positive reactions and which had previously been deemed negative for OvHV-2 by PCR.

887 ## Tables

888 **Tab. 1**. Primer sequences for RLM-RACE

889

Primer	Sequence (5'-3')	Target
5'-RACE outer forward	GCT GAT GGC GAT GAA TGA ACA CTG	5' adapter
5'-RACE inner forward	CGC GGA TCC GAA CAC TGC GTT TGC TGG CTT TGA TG	5' adapter
5'-RACE inner reverse	TGA ATT AGG AGG CGA CCG TA	OvHV2-specific
5'-RACE outer reverse	AGA TTG CCA TCT GGG AGG TT	OvHV2-specific
3'-RACE outer forward	TAC GGT CGC CTC CTA ATT CA	OvHV2-specific
3'-RACE inner forward	GAT GGC AAT CTG CAA CCT TA	OvHV2-specific
3'-RACE inner reverse	CGC GGA TCC GAA TTA ATA CGA CTC ACT ATA GG	3' adapter
3'-RACE outer reverse	GCG AGC AGA ATT AAT ACG ACT	3' adapter

890

891

892 **Tab. 2**. Primer sequences for cloning into pEGFP N3 expression vector and transient

893 expression.

894

Primer	Sequence (5'-3')[a]	Target
Forward Ov8.25 locus	*tcag**g/ctagc***AGTAAGCACACAGAAGGGAG	5' of 8.25 locus with *Nhe*I site
Reverse Ov8.25 locus	*ggac**c/ggccg***GGACACTCATATTAATTAAA ACATTTATTTAC	3' of 8.25 locus with *Eag*I site
Forward Ov8.25 intron	CCTGCTCATAATTATCTTTGCG	5' of first intron
Reverse Ov8.25 intron	TCCTCATCCTCATCTCTCTTCTT	3' of last intron

895 [a] non-OvHV-2 sequences in small letters and italics.

896

897

898 **Tab. 3**. Overview of synthetic constructs.
899

Designation	Description	Purpose
Synthetic Ov8.25 locus	Reverse translated from the native aa sequence as determined from a Swiss cow with MCF, starting from M-codon of the predicted protein and ending prior to the STOP codon. Exon sequences codon-optimized for translation in bovine cells; unaltered introns sequences; additional 5' and 3' nucleotides to provide Restriction enzyme sites for orientation-dependent subcloning	Transient expression of an EYFP-fusion protein; translated from mRNA after splicing
M-less Ov8.25	Same as above but each ATG in the exons of ORF1 replaced by a STOP codon; intron sequences remained native	Transient expression of EYFP without preceding pOv8.25; translated from mRNA after splicing
M-less intron 1 Ov8.25	Shorter version of the above, flanking intron 1	Confirmation of splice sites
M-less intron 2 Ov8.25	Similar as above but flanking intron 2	Confirmation of splice sites
Ov8.25 CDS	Intronless coding sequences of pOv8.25 without STOP codon; codon-optimized for translation in bovine cells	Phenotype of the EYFP-fusion protein in the absence of splicing

900

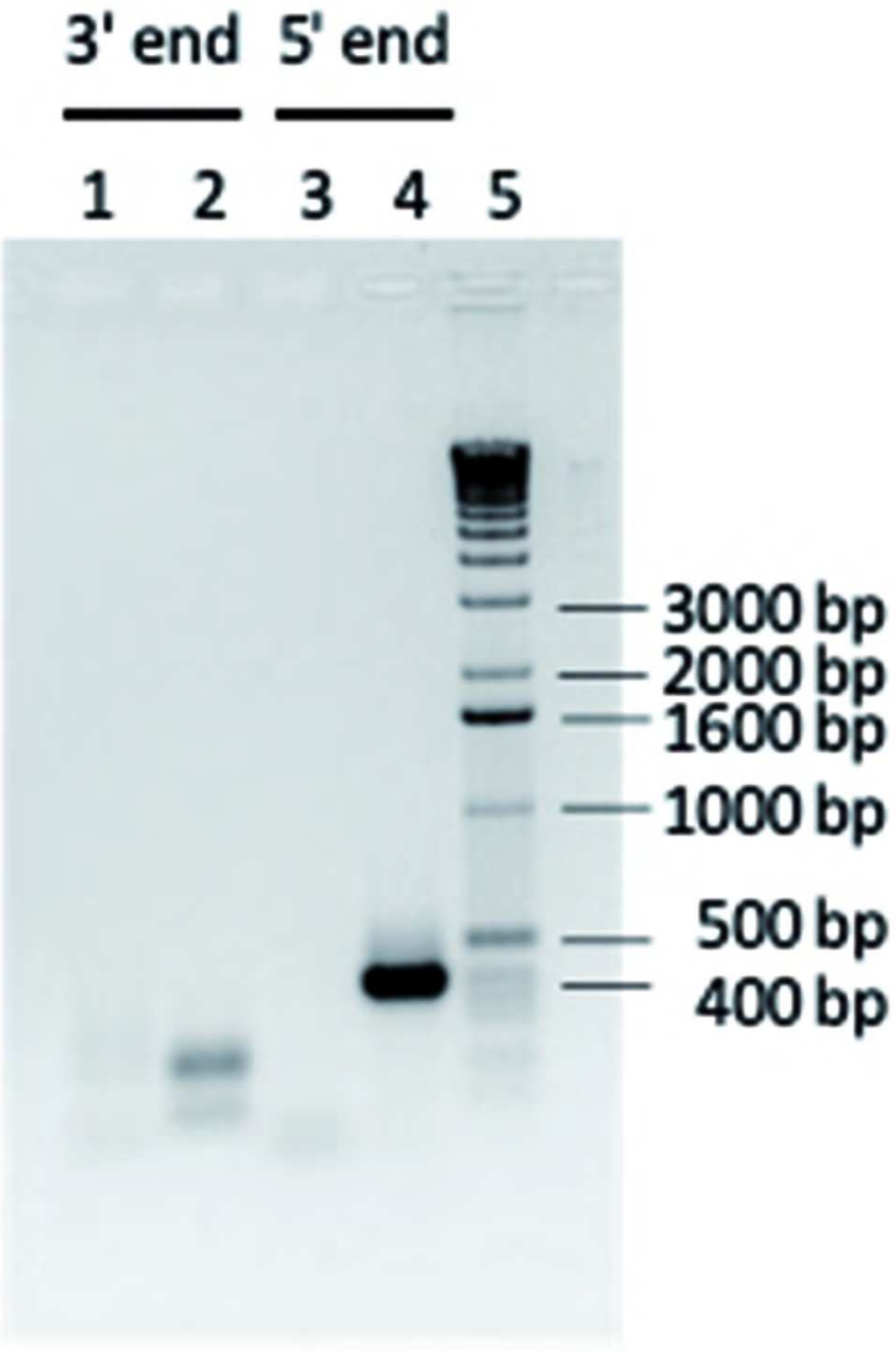

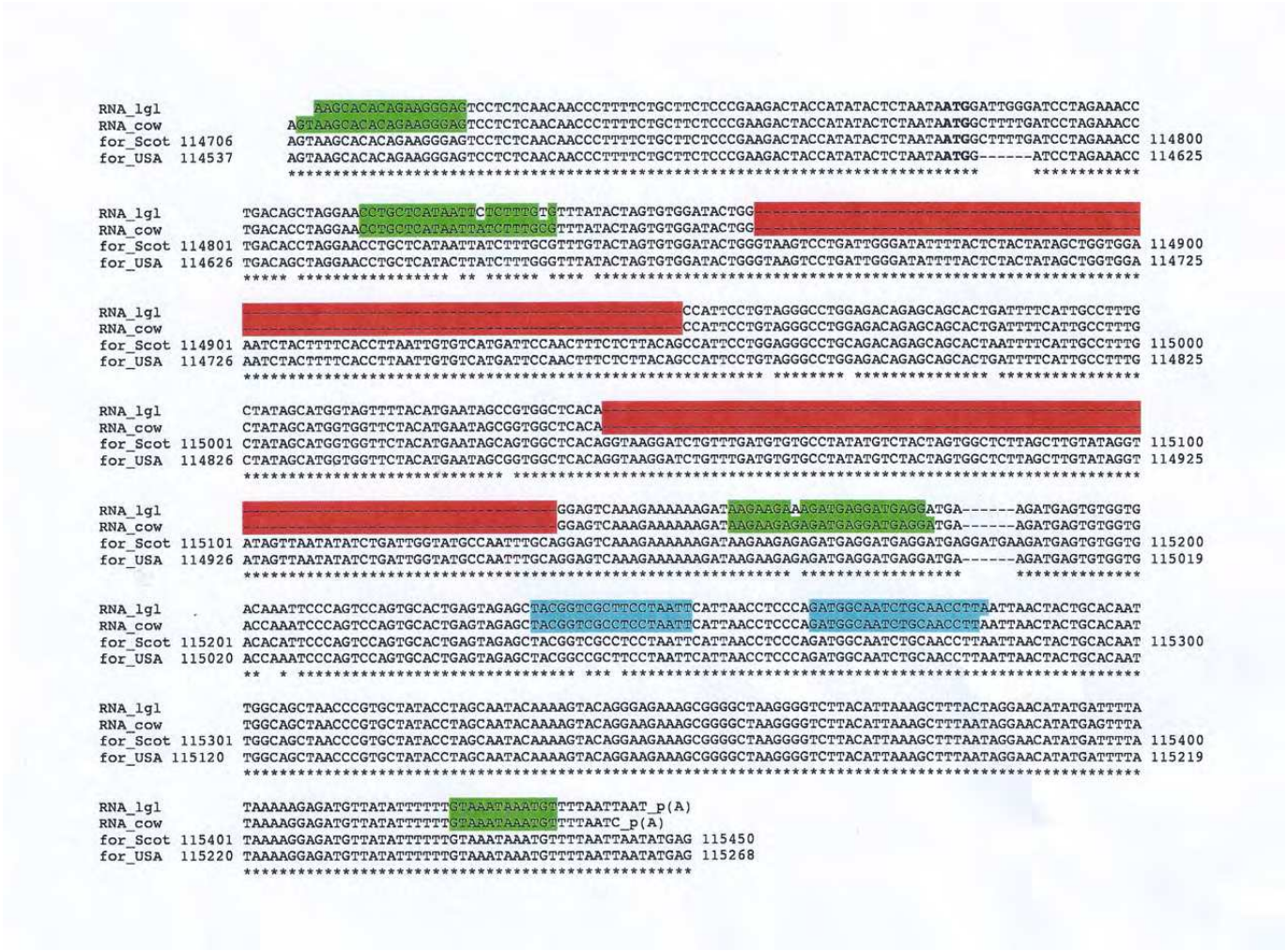

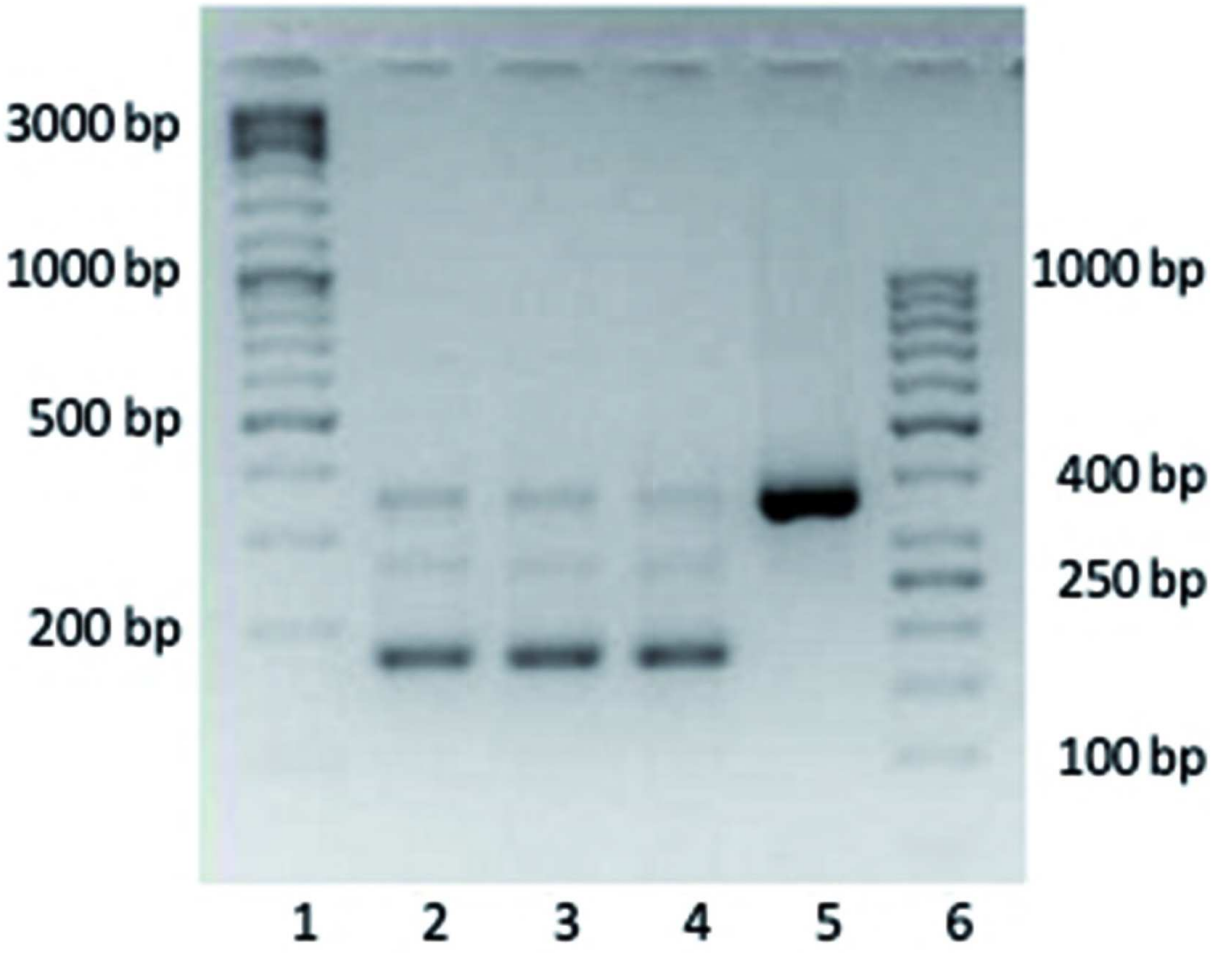

Journal of Virology
JVI
Journal of Virology

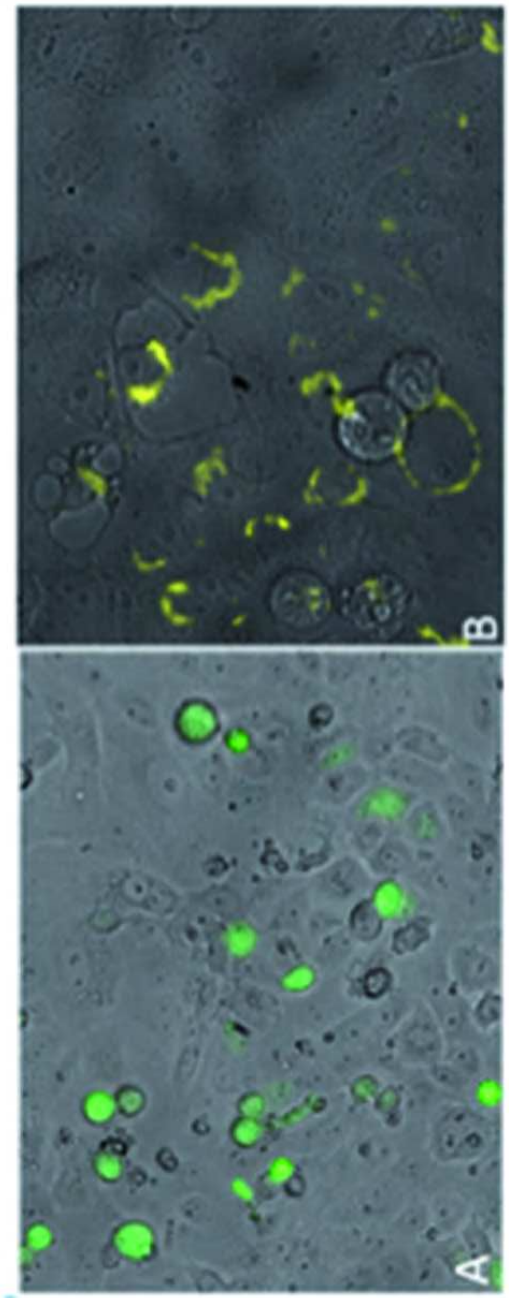

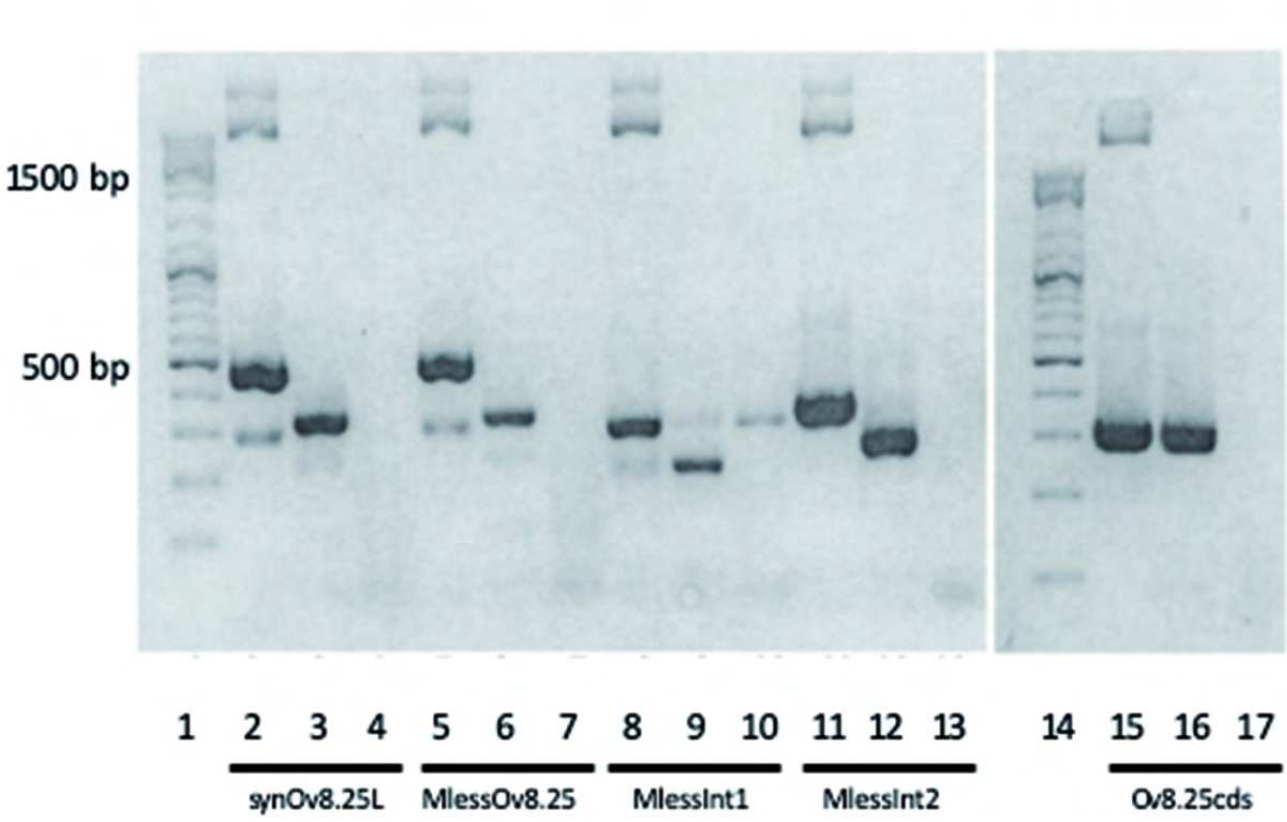

Journal of Virology